

1 Functional Predictors of Causative *Cis*-Regulatory Mutations in 2 Mendelian Disease

3 Hemant Bengani^{1#}, Detelina Grozeva^{2,3#}, Lambert Moyon^{4#}, Shipra Bhatia^{1#}, Susana R
4 Louros^{5,7}, Jilly Hope⁶, Adam Jackson⁵, James G Prendergast⁸, Liusaidh J. Owen¹, Magali
5 Naville⁴, Jacqueline Rainger¹, Graeme Grimes⁶, Mihail Halachev⁶, Laura C Murphy⁶, Olivera
6 Spasic-Boskovic⁹, Veronica van Heyningen¹, Peter Kind^{5,7}, Catherine M Abbott^{6,7}, Emily
7 Osterweil^{5,7}, F Lucy Raymond^{2§}, Hugues Roest Crollius^{4§}, David R FitzPatrick^{1,7§}

8

9 1. MRC Human Genetics Unit, IGMM, University of Edinburgh (UoE) EH4 2XU UK

10 2. Cambridge Institute for Medical Research, University of Cambridge CB2 0XY UK

11 3. Institute of Psychological Medicine & Clinical Neurosciences, Cardiff University CF24 4HQ
12 UK

13 4 Ecole Normale Supérieure, Institut de Biologie de l'ENS, IBENS, 46 rue d'Ulm, Paris, F-
14 75005, France

15 5 Centre for Discovery Brain Sciences, Patrick Wild Centre, University of Edinburgh EH8 9XD
16 UK

17 6. Institute of Genomic and Molecular Medicine, University of Edinburgh EH4 2XU UK

18 7. Simons Initiative for the Developing Brain, University of Edinburgh EH8 9XD UK

19 8. Roslin Institute, University of Edinburgh, EH25 9RG UK

20 9. East Midlands and East of England NHS Genomic Laboratory Hub, Molecular Genetics,
21 Adden brooke's Hospital, Cambridge University Hospitals NHS Foundation Trust CB2 0QQ
22 UK

23 # Joint first authors

24 § Joint senior authors

25

26 **Key words:** Cis-regulatory elements; Enhancer; Repressor; Intellectual Disability; Causative
27 Mutation; X chromosome; FMR1; Zebrafish; Fluorescent transgenic reporters; Genome
28 editing; Mouse embryo; Hindbrain; Hippocampus; Cerebellum; Olfaction; Audiogenic seizures

30 **Abstract**

31

32 Undiagnosed neurodevelopmental disease is significantly associated with rare
33 variants in *cis*-regulatory elements (CRE) but demonstrating causality is challenging
34 as target gene consequences may differ from a causative variant affecting the coding
35 region. Here, we address this challenge by applying a procedure to discriminate likely
36 diagnostic regulatory variants from those of neutral/low-penetrant effect. We identified
37 six rare CRE variants using targeted and whole genome sequencing in 48 unrelated
38 males with apparent X-linked intellectual disability (XLID) but without detectable
39 coding region variants. These variants segregated appropriately in families and altered
40 conserved bases in predicted CRE targeting known XLID genes. Three were unique
41 and three were rare but too common to be plausibly causative for XLID. We compared
42 the *cis*-regulatory activity of wild-type and mutant alleles in zebrafish embryos using
43 dual-color fluorescent reporters. Two variants showed striking changes: one plausibly
44 causative (*FMR1*^{CRE}) and the other likely neutral/low-penetrant (*TENM1*^{CRE}). These
45 variants were “knocked-in” to mice and both altered embryonic neural expression of
46 their target gene. Only *Fmr1*^{CRE} mice showed disease-relevant behavioral defects.
47 *FMR1*^{CRE} is plausibly disease-associated resulting in complex misregulation of
48 *Fmr1*/FMRP rather than loss-of-function. This is consistent both with absence of
49 Fragile X syndrome in the probands and the observed electrophysiological anomalies
50 in the *FMR1*^{CRE} mouse brain. Although disruption of *in vivo* patterns of endogenous
51 gene expression in disease-relevant tissues by CRE variants cannot be used as strong
52 evidence for Mendelian disease association, in conjunction with extreme rarity in
53 human populations and with relevant knock-in mouse phenotypes, such variants can
54 become likely pathogenic.

55 Introduction

56 *Cis*-regulatory elements (CRE; encompassing enhancers and repressors) are genomic
57 sequences that control transcriptional activity of one or more genes on the same
58 chromosome via sequence specific interaction with proteins and/or RNA. CRE can be
59 predicted using comparative genomics,¹ transcriptional characteristics,² patterns of histone
60 modifications and protein association,³ patterns of accessible chromatin,⁴ and direct
61 interactions with promoters⁵. Estimates of the number and nature of CRE in the human
62 genome vary with precise definitions but functional ENCODE data has been interpreted as
63 identifying at least 400,000 putative human enhancers⁶. The role of disrupted CRE function in
64 highly penetrant genetic disease was first recognized in association with structural
65 chromosome anomalies which result in loss or gain of regulatory function through deletion or
66 translocation^{7, 8, 9, 10}. However the identification of disease associated variants within individual
67 CRE has been complicated by several factors. CRE can function over large genomic intervals
68 and the targeted gene may not be the closest gene. Once a target gene assignment is made
69 the existence of shadow CRE (multiple CRE driving similar expression patterns of the same
70 gene),¹¹ can create redundancy and thus tolerance to mutation of individual CRE. A more
71 practical problem is that most CRE exist in the non-coding parts of the human genome where
72 our current understanding of mutation consequence is very incomplete compared to the
73 coding region.

74 Human developmental disorders provide a powerful system for studying the mechanisms
75 underlying genetic disease in general and regulatory mutations in particular. This diverse
76 group of severe and extreme phenotypes have their onset in embryogenesis or early brain
77 development. Developmental disorders are primarily genetically determined with a high
78 proportion of causative variants arising as *de novo* mutations¹². Haploinsufficiency is a
79 common mechanism, which affects many different dosage sensitive genes that show complex
80 patterns of expression during development. The genomic intervals encompassing known
81 developmental disorder genes are commonly enriched in highly conserved CRE¹³. There is
82 evidence of enrichment for *de novo* variants in evolutionarily conserved brain active CRE in
83 severe neurodevelopmental disease at a cohort level,¹⁴ but the confident assignment of
84 variants as causative in affected individuals is difficult¹⁵.

85 Here we have attempted to identify all CRE on the X chromosome and then sequence these
86 in 48 individuals with intellectual disability (ID) and a family history that suggests the disease
87 may be X-linked ID (XLID). All affected individuals were recurrently screened negative for
88 likely causative coding mutations on the X chromosome. Using a rational approach to filtering
89 we identified variants in predicted CRE that are associated with known XLID genes and used
90 a range of *in vivo* assays to find features that discriminate likely neutral from likely causative
91 variants.

92

93

94

95 Results

96 **Selection of study cohort.** In a previous study we have shown that a significant number of
97 individuals with XLID have no likely disease-associated variants in the coding sequence on
98 the X chromosome,¹⁶ and subsequent clinical and research analyses. From this group of
99 undiagnosed individuals we identified 48 unrelated males from families with 3 or more
100 affected members with an inheritance pattern strongly suggestive of XLID (Supplementary
101 **Fig. 1**). We reasoned that this cohort should be enriched for regulatory mutations. These
102 families also increase the prior probability that any causative CRE variants would be on the X
103 chromosome thus significantly reducing the genomic search space for interrogation.

104

105 **Identification of cis-regulatory enhancers on the X chromosome (chr X).** We have
106 previously identified >100,000 putative CRE covering 4.4% of the human X chromosome and
107 assigned the likely target gene using evolutionary conservation of linkage between CRE and
108 genes located within 1.5 Mb of each other¹⁷. Approximately a third of CRE could be assigned
109 to a single gene with the remainder having more than one equally plausible target. 389/812
110 protein coding genes on the X chromosome could be assigned to at least one CRE.
111 Chromatin immunoprecipitation for H3K4me1 in human developing brain showed 10-fold
112 enrichment of these putative CRE. Fluorescent reporter transgenic zebrafish showed >60% of
113 the ~1000 analyzed CRE drive expression in a pattern that overlaps that of endogenous gene
114 activation during development¹⁷.

115

116 **Targeted sequencing and variant filtering of chrX coding regions and enhancers.** In the
117 present study we used a targeted sequencing approach to identify variants within all coding
118 regions and CRE on the X chromosome that may be causing XLID in the 48 families using a
119 custom 15.9 Mb oligonucleotide pull-down consisting of 227323 baits. A total of 40,699
120 variant calls passed basic quality controls in these individuals (**Fig. 1a**). As expected, no
121 clearly disease-associated variants were identified in the coding exons in any of the
122 probands. 628 rare/ultrarare hemizygous variants were identified in high confidence putative
123 CRE of which 31 altered highly conserved bases in enhancers that were predicted to control
124 known XLID genes. 30/31 were confirmed by Sanger sequence analysis in the probands but

125 only 6 of these 30 were shown to segregate appropriately in the XLID families using samples
126 from additional affected, unaffected males and obligate females (**Fig.1b**). Details of
127 segregation in pedigrees are shown in (Supplementary **Fig. 1 & Supplementary Table 4**).
128 4/48 probands carried one of these six variants and 1/48 carried two.

129

130 **Allele frequencies to assess the plausibility of each rare variant being causative.** The
131 position and gnomAD variant allele frequencies (AF) of these six variants are shown in
132 (Supplementary **Table 5**). We used the approach of Whiffin et al,¹⁸ to calculate the maximum
133 plausible allele frequency for a causal variant in any of the CRE. We chose very conservative
134 parameters: 0.01 for genetic heterogeneity (i.e. 1% of all undiagnosed XLID is caused by a
135 variant in one CRE), 0.2 for allelic heterogeneity (i.e. only 5 different causative variants can
136 exist per CRE) and 0.5 for penetrance (complicated by X-linked inheritance but likely to be ~1
137 in males and ≥ 0.1 in females). These parameters gave maximum permitted 95% confidence
138 AF = $4e06$. Three of the five individuals (S3, S19 and S43) with CRE variants that survived
139 initial filtering do carry variants that may be plausibly disease associated on the basis of the
140 gnomAD AF. The single variant in S31 and both variants in S24 were confirmed to be rare but
141 have gnomAD AF that are too common to be likely disease associated.

142

143 **Reporter transgenic analysis of rare filtered variants segregating with the disorder.** The
144 reference and alternative base versions of all six rare or ultrarare CRE variants were then
145 tested for CRE function using dual-color fluorescent transgenic assay in zebrafish¹⁹. In these
146 experiments the mutant CRE drives expression of one fluorescent protein and the wild-type
147 CRE controls a different fluorescent protein in the same fish. Multiple stable lines are
148 created, expression domains are scored and only consistent differences between the
149 reference and alternative alleles are taken as evidence of a functional effect of the mutation.
150 Only two variants in the CRE controlling the XLID genes (in two different probands),
151 *TENM1*^{CRE} and *FMR1*^{CRE}, demonstrated a consistent restriction of expression of reporter
152 gene in brain as a result of the variants (**Fig. 2c, d, 3c, d**). The domain of expression of the
153 reporter gene driven by *TENM1*^{CRE} and *FMR1*^{CRE} overlap with the expression domain of the
154 target gene in zebrafish respectively (Fig. 2a, 3a).

155

156 ***TENM1*^{CRE} creates a de novo and functionally repressive binding site for *six3*.** We had

157 noted that the *TENM1*^{CRE} variant created a predicted binding site for the homeodomain-

158 containing DNA binding proteins SIX3 or SIX6 in the human element (Fig. 2b). We chose

159 SIX3 for further study as it is essential for early brain development and with pathway-specific

160 activator and repressor activity²⁰. To determine if SIX3-mediated repression may be

161 responsible for the altered enhancer activity in the variant *TENM1*^{CRE} we titrated morpholinos

162 against zebrafish *six3* into the embryos from a *TENM1*^{CRE} dual color fluorescent transgenic

163 line to the point where there was no morphological anomaly. This resulted in an alteration in

164 the expression of the *TENM1*^{CRE} transgene to match the wildtype in the morphant embryos

165 (Fig. 2e, f), supporting acquisition of SIX3 repression as the mechanism for the transcriptional

166 effect in zebrafish embryos.

167

168 ***Fmr1* expression and behavioral phenotypes in *Fmr1*^{CRE} and *Tenm1*^{CRE} mouse models.**

169 CRISPR/Cas9 genome editing was used to knock the exact mutation into mouse embryos via

170 homologous recombination for both variants that showed a consistent functional

171 consequence in the zebrafish lines: *FMR1*^{CRE} and *TENM1*^{CRE}. We established multiple

172 independent mouse lines for each CRE variant on a C57BL/6 background (Fig. 2b, 3b). All

173 lines resulted in hemizygous mutant animals, at the expected ratio that were healthy and

174 fertile with no obvious morphological abnormalities. We first looked for alteration in the

175 expression of the predicted target gene during development. *Tenm1*^{CRE} resulted in loss of

176 expression in the hindbrain of the mutant embryos using whole-mount *in situ* hybridization

177 (WISH) for the endogenous gene (Fig. 2g, 2h). *Fmr1*^{CRE} caused a significant reduction in the

178 developmental expression of *Fmr1* in the olfactory placodes and the forebrain (Fig. 3e). Both

179 variants have an effect on endogenous gene expression i.e. neither is behaving as a shadow

180 CRE.

181 To look for functional phenotypic effects segregating with either CRE variant we first tested

182 olfaction. This sense was selected for two reasons. First, the complete loss of *Fmr1*

183 expression in the olfactory placode in *Fmr1*^{CRE} embryos. Secondly, *TENM1/Tenm1* mutations

184 have recently been identified in humans and mice associated with congenital generalized

185 anosmia²¹. Using a buried chocolate button test hemizygous *Fmr1*^{CRE} mice showed a
186 significant increase in time to discovery compared to wild-type male littermates (**Fig. 4g**).
187 *Tenm1*^{CRE} hemizygotes had olfactory function similar to wild-type male littermates (**Fig. 4h**).

188

189 **Abnormal hippocampal protein synthesis and electrophysiology in *Fmr1*^{CRE} mice**

190 *FMR1/Fmr1* encodes 516-622 amino acid RNA-binding and polyribosome associated protein
191 isoforms (FMRP) that are essential for the normal development and function of neurons in the
192 brain. Loss of FMRP function is responsible for Fragile X syndrome, the most common form
193 of XLID. A well-characterised biochemical effect of loss of FMRP in the brain of the mouse
194 model of Fragile X syndrome is the mGluR5- or ERK1/2-dependent elevation of basal protein
195 synthesis²². We found a significant increase in bulk protein translation levels in tissue slices of
196 dorsal hippocampus of *Fmr1*^{CRE} mutant male mice compared to wild-type male littermates
197 (**Fig. 4b**). This would be consistent with the reduction of *Fmr1* expression we observed in
198 mutant embryos (**Fig. 3e**). Importantly we did not find significant difference in the expression
199 of *Fmr1* transcript in *Fmr1*^{CRE} mutant male mice compared to wild-type male littermates at
200 developmental stage P-7 (by qPCR), P-14 (by qPCR) (**Supplementary Fig. 2**) or P-25 (by
201 RNAScope) (**Fig. 4c,d,e**) and (by RNA Sequencing) (**Supplementary Fig. 3**).

202 Given the gene expression results, it was surprising to find an increase in FMRP protein
203 abundance in the hippocampus of *Fmr1*^{CRE} mutant male mice as compared to wild-type litter
204 mates using western Blotting (**Fig. 4a, b; Supplementary Fig. 4**). The increase in FMRP
205 protein levels is consistent with our finding that mGluR-dependent long-term depression
206 (LTD) in the CA3-CA1 regions of the mouse hippocampus is significantly decreased in
207 *Fmr1*^{CRE} hemizygous mutant male mice as compared to wild-type litter mates (**Fig. 4f**) as this
208 is exaggerated in *Fmr1*-null animals²³. *Fmr1*^{CRE} hemizygous mutant mice were also found to
209 have no increase in audiogenic seizure predisposition, a phenotype that typifies *Fmr1* null
210 mice (**Fig. 4i**). These latter three key features strongly suggest that *Fmr1*^{CRE} does not
211 represent a simple loss of FMRP function.

212

213 **Clinical re-evaluation and whole genome sequencing of individuals carrying**

214 ***FMR1*^{CRE}**. Re-evaluation of affected individuals within the family in which *FMR1*^{CRE} is

215 segregating (Fig. 4j) revealed no features suggestive of a Fragile X (FRAX) syndrome
216 diagnosis (OMIM #300624); FMRP deficiency) other than macrocephaly and intellectual
217 disability. Importantly none of the individuals carrying $FMR1^{CRE}$ showed clinical features of
218 FRAX Tremor and Ataxia Syndrome (FRAXTAS [OMIM #300623]; FMRP over-
219 production)²⁴. Whole genome sequencing of individual S3 ($FMR1^{CRE}$ proband) did not identify
220 any other plausible cause of his intellectual disability.
221

222 Discussion

223

224 The motivation for initiating this study was the difficulty in assigning pathogenic or likely
225 pathogenic status to a *de novo* or segregating variant in a regulatory sequence. Currently
226 almost all such ultra-rare variants would be considered of uncertain significance using current
227 best practice guidelines^{25, 26}. However it has been shown that using "well-established"
228 functional assays demonstrating a variant has abnormal gene function (coded as assigning
229 PS3 in the guidelines) has the potential to change many variants of uncertain significance
230 (VUS) to likely pathogenic status²⁷. The question then becomes: how should we use data from
231 functional assays in clinical interpretation of regulatory variants. Given the rapid switch from
232 targeted whole exome sequencing to whole genome sequencing it is likely that there will be
233 an increasing need to develop a rational approach to the interpretation of ultra-rare regulatory
234 variants.

235 Here we attempted to perform an integrated clinical, genetic, developmental, behavioural and
236 neurophysiological approach to the analyses of CRE variants identified in a cohort of affected
237 individuals with a Mendelian phenotype that should be enriched for causative cis-regulatory
238 mutations. XLID accounts for ~16% of ID in males²⁸. Mutations in the coding region of at least
239 81 different genes,^{16, 29} have been identified as causing XLID. Given the significant
240 contribution of XLID to ID and the observed regulatory variant enrichment in a large cohort of
241 individuals with neurodevelopmental disorders,¹⁴ we reasoned that we could increase the
242 prior probability of identifying likely causative mutations by restricting the genomic search
243 space to the X chromosome and by limiting our investigations to variants in enhancers that
244 targeted known XLID genes. This strategy was implemented as most known disease-
245 associated regulatory mutations were identified because they partially,³⁰ or fully,³¹ phenocopy
246 loss-of-function mutations in the target gene. If true for our cohort, then matching the pattern
247 of clinical features of individuals carrying a specific regulatory mutation to those of the
248 syndrome associated with intragenic mutations would have diagnostic value.

249 One important feature of our study was that we could compare the functional impact of
250 variants which were plausibly responsible for a significant Mendelian disorder and those that
251 were too common to be disease associated using established statistical approach¹⁸. The *in*
252 *vivo* analysis of the *TENM1* enhancer was particularly interesting in this regard. Both the

253 transgenic zebrafish embryos and knock-in mouse lines showed clear evidence of
254 abnormality in developmental gene expression. Indeed, we were able to identify the
255 transcription factor mediating the repressive effect of the rare CRE variant in zebrafish. This
256 could be taken as strong evidence of disease association if the significance of the allele
257 frequency was not appreciated. It seems likely that simpler and more commonly used *in vitro*
258 assays of enhancer activity,³² will be more prone to “over-reporting”. It is also clear that most
259 unique variants will also be neutral or of low-penetrant effect so the allele frequency on its
260 own is not sufficient for discrimination in clinical analysis.

261 The unique CRE variant *FMR1*^{CRE} is the most plausible disease associated allele of those
262 identified in this study. This variant produced abnormal embryonic expression of endogenous
263 *Fmr1* in the mouse model (**Fig. 3e**). The reporter transgenic analysis in zebrafish also
264 showed an expression pattern that would be consistent with tissue specific loss of function
265 during early brain development. In contrast, we were unable to show evidence of significant
266 transcriptional misregulation in the *Fmr1*^{CRE} post-natal brain using qRT-PCR (Supplementary
267 **Fig. 2**), RNA-Seq (Supplementary **Fig. 3**) or RNAscope *in situ* hybridization (**Fig. 4d, e**). This
268 was particularly interesting in the context of the other analyses that we performed in P25
269 *Fmr1*^{CRE} mice. First the pattern of bulk protein synthesis was similar to that seen in *Fmr1* KO
270 mice. However, the direction of electrophysiological change of LTD was opposite from *Fmr1*
271 KO mice and increased levels of FMRP protein were observed (**Fig. 4a, b**; Supplementary
272 **Fig. 4**). These apparently paradoxical results may be the consequence of developmental
273 mis-programming of the cells in the hippocampus. In the future we intend to employ single
274 cell transcriptomics and ATAC-Seq to test this hypothesis.

275 We chose the buried food behavioural assay to assess olfaction because this would be
276 plausibly disrupted in both *Tenm1*^{CRE},²¹ and *Fmr1*^{CRE}.^{33, 34} Like all mouse behavioural assays
277 this is very likely to be influenced by other neurodevelopmental and environmental factors.
278 That said, the fact that it was normal in *Tenm1*^{CRE} and impaired in *Fmr1*^{CRE} is probably
279 significant given the striking loss of *Fmr1* expression in the olfactory placodes in *Fmr1*^{CRE}
280 embryonic mice. Surprisingly, given the human phenotype, it has been difficult to identify any
281 behavioural assay that provides consistent evidence of cognitive impairment in *Fmr1* KO
282 mice³⁵.

283 For the reasons outlined in the two paragraphs above we do not consider it to be surprising
284 that the proband S3 and his affected male relatives carrying $FMR1^{CRE}$ do not show a clinical
285 pattern typical of either Fragile X syndrome [OMIM 300624] or FRAXTAS [OMIM 300623].The
286 family presented with a non-specific intellectual disability associated with mild macrocephaly.
287 We consider it likely that many disease associated CRE variants will result in clinical features
288 that significantly differ from those seen associated with intragenic mutations of target gene. If
289 this heterogeneity in clinical features is indeed true, the clinical genetics field will have
290 relatively limited ability to predict the phenotypes associated with regulatory mutations even
291 when the clinical impact of intragenic mutations of target gene are well characterised.
292 We can conclude that although it remains challenging to recognise highly penetrant CRE
293 causative variants, the population allele frequency estimates from gnomAD 2.1.1 has power
294 to identify those of neutral or low penetrant effect. These data allowed us to class $TENM1^{CRE}$
295 as implausible as an XLID causative variant despite it being in an evolutionarily conserved,
296 non-redundant CRE with a strong repressive effect on *Tenm1* expression during mouse
297 hindbrain development. The discriminative power of the extreme rarity of individual alleles
298 may prove particularly useful for the identification of causative variants in CRE which are
299 poorly conserved across species but under high levels of selective constraint within human
300 populations³⁶.For the time being we suggest that causative variants are restricted to those
301 with strong human genetic evidence, supported by modelling of the precise variant *in vivo* and
302 resulting in both transcriptional misregulation and phenotypic effect.

303

304 **Materials and methods**

305

306 **Cohort Selection.** Genomic DNA samples from 48 individuals (probands) with moderate-to-
307 severe intellectual disability (ID) were used in this study. The appropriate research ethical
308 approval was obtained (IRAS 03/0/014), and parents or guardians provided informed written
309 consent. Each individual is assumed to have X-linked recessive form of ID on the basis of
310 positive family history: three or more cases of ID in males only, predominant sparing of carrier
311 females and no evidence of male-to-male transmission of the disease (Supplementary Fig. 1).
312 A clinical geneticist had assessed the individuals and the cause of the ID was unknown. The
313 severity of the disease was categorized using DSM-IV or ICD-10 classifications (profound

314 mental retardation was classified as severe). The patients had previously been tested
315 negative by routine diagnostic approaches (i.e., CGH microarray analysis at 500 kb
316 resolution, fragile X [MIM #300624], methylation status of Prader Willi [MIM
317 #176270]/Angelman syndrome [MIM #105830]). In addition, coding variants on the X
318 chromosome likely to lead to disease have not been found within a previous study¹⁶.

319

320 **Targeted Capture Design and Sequencing.** A comprehensive list of coordinates of all the
321 exonic and conserved regulatory elements from human X chromosome was used to design a
322 customized capture library from Roche, NimbleGen (Supplementary Table 1). Library
323 preparation, pre and post capture multiplexing were performed using the SeqCap EZ Choice
324 XL kit (Roche NimbleGen) and TruSeq index barcodes (Illumina) were used according to the
325 manufacturer's instructions. 4 different DNA samples were pooled for pre capture multiplexing
326 and 4 post captured libraries were combined and paired-end sequenced performed on a
327 single lane of a HiSeq-2000 instrument (Illumina). In total 16 different DNA samples were
328 sequenced in a single lane of a HiSeq-2000 and 4 lanes were used to sequence all the 48
329 DNA samples.

330

331 **Read Mapping, Variant Analysis and Enhancer Selection.** Following quality control with
332 FastQC, reads were mapped to the GRCh37 version of the human reference genome using
333 BWA³⁷. Variants were called using GATK,³⁸ according to its recommended best practice
334 pipeline. 40,699 variants remained after filtering out variants that failed GATK's variant quality
335 score recalibration. These variants were subsequently compared to dbSNP v137 to filter out
336 common variants. Any variant with one of the following handles in dbSNP (1000GENOMES,
337 CSHL-HAPMAP, EGP_SNPS, NHLBI-ESP, PGA-UW-FHCRC) were excluded where the
338 variant's reported minor allele frequency was greater than 0.01 and the minor allele was
339 reported to be observed in at least two samples. The remaining 9,577 X chromosome
340 variants were then annotated with SnpEff,³⁹ to determine their predicted effects on genes.
341 gnomAD 2.1 allele frequencies were documented for the surviving variants. To determine the
342 best candidates for experimental validations, the variants were ranked based on extreme
343 evolutionary conservation. Using Multiple Sequence Alignments from 45 vertebrate species

344 against the Human genome (UCSC genome browser), mutations were retained if the
345 reference human allele was conserved in at least 90% of the species, and then sorted by
346 decreasing conservation depth. Top variants were then manually evaluated using biochemical
347 signals from the ENCODE project (H3K4me1, H3K4me3, H3K27ac, DNase1 sensitivity), and
348 based on the association to target genes known to be responsible for XLID or functionally
349 related to brain development, leading to a final selection of 31 candidate variants
350 (Supplementary **Table 4**). Target genes for each of the CRE harbouring the variants were
351 assigned as described previously¹⁷. Motif search on CRE element was performed on a 40bp
352 window around the mutated base for both human and mouse sequences using the FIMO
353 software from the MEME suite⁴⁰. The motif databases used for the search were Jaspar Core
354 2018 for vertebrates and Uniprobe mouse motifs as downloaded from the MEME website.
355 Motifs with a p-value of 0.001 or lower that were present uniquely in either the WT or the
356 mutant sequences are reported.

357

358 **Transgenic Zebrafish, In Situ Hybridization (ISH) and Morphant Generation.** All mouse
359 and zebrafish experiments were approved by The University of Edinburgh ethical committee
360 and performed under UK Home Office license number PIL 60/12763, 70/25905, I655D57B6,
361 PA3527EC3 and 1724D1B2C; PPL 60/4418, 60/4424, IFC719EAD and 60/4290. The wild
362 type and mutant versions of the *FMR1*^{CRE} and *TENM1*^{CRE} were analyzed for their regulatory
363 activities in dual color enhancer-reporter transgenic assays in zebrafish embryos¹⁹. The
364 sequences of the primers used in generating the constructs utilized in the assay are listed in
365 (Supplementary **Table 2**). A summary of the number of independent lines analyzed for each
366 enhancer and their expression sites is included in (Supplementary **Table 3**). The transgenic
367 F1 embryos were processed for imaging as described¹⁹. The images were taken on a Nikon
368 A1R confocal microscope and processed using A1R analysis software. A zebrafish *six3*
369 antisense morpholino oligonucleotide (Six3AMO) was obtained from Gene Tools, LLC, with
370 the following sequence: 5' GCTCTAAAGGAGACCTGAAAACCAT 3'. This morpholino has
371 sequence complementary to the highly conserved sequences around the translation initiation
372 codon of both *six3a* and *six3b*, and hence inhibits the function of both zebrafish *six3*
373 genes⁴¹. As control we used the Gene Tools LLC standard negative control morpholino: 5'

374 CCTCTTACCTCAGTTACAATTTATA 3'. The morpholinos were injected into 1 to 2-cell stage
375 of at least 100 embryos to deliver an approximate amount of 2.5 ng per embryo. RNA in situ
376 hybridization on fish embryos was performed as previously⁴². The sequences of primers used
377 for synthesis of specific probes are listed in (Supplementary **Table 2**).

378

379 **Generation of Transgenic Mice and Embryo ISH.** CRISPR/Cas9 gene targeting technology
380 was used to generate mouse lines with orthologous mutations; *Fmr1*^{CRE} and *Tenm1*^{CRE}.
381 Double stranded DNA oligomer that provides a template for the guide RNA sequence was
382 cloned into px461. The details of guide RNA and repair template sequence are in
383 **Supplementary note**. The full gRNA template sequence is amplified from the resulting px461
384 clone using universal reverse primer and T7 tagged forward primers. The guide RNA PCR
385 template is used for *in vitro* RNA synthesis using T7 RNA polymerase (Neb), and purified
386 using RNeasy mini kit (Qiagen) purification columns. The zygotic injection mix contains Cas9
387 mRNA (Tebu Bioscience @ 50ng/μl), guide RNA (25ng/μl) and repair template single
388 stranded DNA (IDT 150ng/μl). Injected embryos were transferred into the oviducts of pseudo-
389 pregnant females to litter down. Genotyping of the resulting mice was performed by Sanger
390 sequencing using tail tip DNAs. F0 mice with desired variant were crossed with C57BL/6 to
391 generate a stable mice line. *In situ* hybridization on mouse embryos was performed with DIG-
392 labelled gene-specific antisense probes as previously described⁴³. The sequences of primers
393 used for synthesis of specific probes are listed in (Supplementary **Table 2**).

394

395 **Behavioral Testing of *Fmr1*^{CRE} and *Tenm1*^{CRE} Mouse Lines.** Male WT (wild type) and
396 mutant (*Fmr1*^{CRE} and *Tenm1*^{CRE} knock-in) littermates were used for the test at P25-32 using
397 the buried food test assay. For three consecutive days before the test, ¼ Cadbury's chocolate
398 button was placed in the home cage for 15 minutes to habituate the mice to the food reward.
399 12 hours before the test, all food was removed from the home cage to motivate the mouse to
400 find the food reward during the test. After 12 hours, the mouse was placed in a clean cage
401 with fresh bedding in which ¼ chocolate button had been buried 1cm beneath the bedding.
402 The time taken for the mouse to find the buried food was scored and the test was stopped if
403 the mouse did not find the food after 15 minutes. The bedding was replaced and the cage

404 cleaned with 1% Conficlean between mice. All mice were scored blind to the genotype.
405 Unpaired t-tests were used to determine statistical significance.

406

407 **Seizure Propensity Testing of *Fmr1*^{CRE}.** Male WT and *Fmr1*^{CRE} knock-in mutant littermates
408 (P25-32) were tested for audiogenic seizures as described previously⁴⁴. Briefly, animals were
409 transferred to a transparent plastic test chamber and, after 1 minute of habituation, exposed
410 to a 2 min sampling of a modified personal alarm held at > 130dB. Seizures were scored for
411 incidence (seizure/no seizure) and severity, with an increasing scale of 1=wild running,
412 2=clonic seizure, and 3=tonic seizure. All mice were tested and scored blind to genotype.
413 Statistical significance for incidence was determined using two-tailed Fisher's exact test.

414

415 **Basal Protein Synthesis and FMRP Western Blotting.** Protein synthesis levels were
416 measured following the protocol outlined by Osterweil²². The detailed protocol is described in
417 the **Supplementary note**.

418 For western blots, forebrain, midbrain and hindbrain from (P-14) and hippocampal slice from
419 P-25 male WT and *Fmr1*^{CRE} knock-in mutant littermates were dissected and homogenized in
420 lysis buffer (20 mM HEPES pH 7.4, 0.5% Triton X-100, 150 mM NaCl, 10% glycerol, 5 mM
421 EDTA with protease inhibitor cocktail (Roche), incubated at 4 °C for 30 min followed by
422 centrifugation at 14000 rpm for 30 min to collect the supernatant. These samples were
423 directly used for SDS-PAGE and transferred onto nitrocellulose membranes for immunoblot
424 analysis with FMR1 (MAB2160, Milipore) and Actin antibodies (13E5, CST).

425

426 **Hippocampal Slice Electrophysiology.** Electrophysiology experiments were performed as
427 outlined by Stephanes⁴⁵. The detailed protocol is described in the **Supplementary note**.

428

429 **RNAscope Assay and Imaging.** In situ RNA hybridization was performed using the
430 RNAscope assay (Advanced Cell Diagnostics, ACD, Hayward, CA, USA) according to the
431 manufacturer's recommendations. The detailed protocol is described in the Supplementary
432 note. The images of sections were processed using the multimodal Imaging Platform
433 Dragonfly (Andor Technologies, Belfast, UK) using air 40x Plan Fluor 0.75 DIC N2. Data were

434 collected in Spinning Disk 25 μm pinhole mode on the high sensitivity iXon888 EMCCD
435 camera. According to Advanced Cell Diagnostics, each mRNA molecule hybridized to a probe
436 appears as separate small puncta. Data visualization and spot counting was done using
437 IMARIS 8.4 (Bitplane).

438 ***Acknowledgements***

439 DRF and VvH were supported by MRC University Unit grant to the MRC Human Genetics
440 Unit at the University of Edinburgh. HB & MN and project costs were supported and funded
441 by the 7th framework programme of the European Union [NeuroXsys Project HEALTH- F4-
442 2009-223262]. HB was subsequently funded by a grant from NewLife (Grant Ref: 14-15/07).
443 National Institute of Health Research Bioresource for Rare Diseases (grant number
444 RG65966) for whole genome sequence data from 12,596 X chromosome alleles as controls.
445 JH is funded by a BBSRC studentship. FLR and DG are funded by NIHR Cambridge
446 Biomedical Research Centre grant. HRC received support from the French Government from
447 programs implemented by ANR with the references ANR-10-LABX-54 MEMOLIFE and
448 ANR-10-IDEX-0001-02 PSL* Research University. DRF,PK and EO receive grant funding
449 from the Simons Initiative for the Developing Brain.

450

451 ***Author Contributions***

452 DRF, HRC, FLR and VvH conceived the project and with CA and EO designed the
453 experimental approaches. HB, DG, OSB, SB, SRdL, JH and SB performed the experiments
454 and interpreted the results. LM, MN and HRC performed the computational genomic analysis.
455 DRF, HRC and FLR wrote the manuscript with contributions from HB, SB, EO and VvH.

456

457 **Figure Legends**

458 **Fig. 1:**

459 **Identification and filtering of XLID-associated regulatory variants and their predicted**

460 **target genes. a.** Workflow of the sequencing and curation pipeline leading to the

461 identification of six XLID-associated CRE variants in five probands. **b.** Schematic showing the

462 genomic region of the six genomic variants in the five probands (S19, S24, S3, S43, S31)

463 indicating the location of the XLID-associated CRE variants along with the gnomAD

464 frequencies and their predicted target genes (indicated in red, genomic coordinates from

465 h19/GRCh37 genome build).

466

467 **Fig. 2:**

468 **TENM1 associated regulatory variant alters the expression of *Tenm1* in mouse**

469 **embryonic development. a.** *mRNA in situ* hybridization showing expression of *tenm1* in

470 midbrain, hindbrain and neural tube during embryonic development in wild type zebrafish. **b.**

471 **Human and mouse ($TENM1^{CRE}/Tenm1^{CRE}$) sequences are shown with the variant base**

472 **marked in blue, resulting in gain of SIX3/SIX6 and HDX binding sites in $TENM1^{CRE}$ and**

473 **Six6 and Hdx binding sites in *Tenm1*^{CRE}.c-d.** Dual color fluorescent transgenic assay in

474 zebrafish with wild-type (Wt) and mutant $TENM1^{CRE}$ driving eGFP and mCherry expression

475 respectively. Loss of enhancer activity is observed in midbrain and hindbrain with the mutant

476 $TENM1^{CRE}$ allele. **e-f.** *six3* knockdown rescues the effect of the mutant variant on the activity

477 of $TENM1^{CRE}$. Control morpholino injected embryos show loss of reporter activity in midbrain

478 and hindbrain by mutant allele, where the mutation creates a Six3 binding site (e).

479 Knockdown of *Six3* rescues the activity of mutant allele in the midbrain and hindbrain (f). **g-h.**

480 Whole-mount *in situ* hybridization for *Tenm1* shows loss of expression of *Tenm1* in the

481 hindbrain and midbrain of $Tenm1^{CRE}$ mutant embryos as compared to wild-type embryos.

482 MB: Midbrain; HB: Hindbrain; NT: Neural tube; hpf: hours post fertilization

483

484

485

486 **Fig. 3:**

487 **FMR1 associated regulatory variant alters the expression of *Fmr1* in mouse embryonic**
488 **development. a.** mRNA *in situ* hybridization showing expression of *fmr1* in forebrain and
489 midbrain during embryonic development in wild-type zebrafish. b. **Human and mouse**
490 **(*FMR1*^{CRE}/*Fmr1*^{CRE}) sequences are shown with the variant base marked in blue,**
491 **resulting in loss of RFX2/Rfx2 binding site in *FMR1*^{CRE}/*Fmr1*^{CRE}.** c-d. Dual color
492 fluorescent transgenic assay in zebrafish with wild-type (Wt) and mutant (Mut) *FMR1*^{CRE}
493 driving eGFP and mCherry expression respectively. Loss of enhancer activity is observed in
494 forebrain with the mutant *FMR1*^{CRE} allele. e. Whole-mount *in situ* hybridization for *Fmr1* shows
495 loss of expression of *Fmr1* in the nasal placode and midbrain *Fmr1*^{CRE} mutant embryos as
496 compared to wild-type embryos.

497 FB: Forebrain; MB: Midbrain; TG: Trigeminal ganglia; NP: Nasal placode; hpf: hours post
498 fertilization

499

500 **Fig. 4:**

501 **Functional phenotypic effects observed in mice bearing *FMR1* associated regulatory**
502 **variant.** a) Levels of FMRP protein observed in the forebrain, midbrain and hindbrain of
503 *Fmr1*^{CRE} knock-in mutant mice as compared to wild-type litter mates at P-14. b) Significant
504 increase in bulk protein synthesis levels in slices from dorsal hippocampus of *Fmr1*^{CRE} knock-
505 in mutant male mice as compared to wild-type male littermates. c) H&E stained brain sagittal
506 section with marked hippocampus regions is shown as reference image on which RNAscope
507 analysis was done *Fmr1*^{CRE} mutant male mice compared to wild-type male littermates.
508 Images of RNAscope processed CA3-CA1 components of the hippocampus brain section
509 were taken as shown by numbers (1-8) starting from dentate gyrus (DG). d) Reference image
510 of RNAscope processed section with *Fmr1* transcript (Red), *Pax6* transcript (Green) and
511 nucleus (Blue/DAPI). Each transcripts are represented by spots. e) Graphical representation
512 of *Fmr1* transcripts normalised to *Pax6* transcripts (used as control) is shown across the
513 whole CA3-CA1 components of the hippocampus brain section between *Fmr1*^{CRE} mutant
514 male (purple) mice compared to wild-type littermates (orange). No significant difference was
515 observed in the *Fmr1* transcripts level across the whole region used for analysis. f). mGluR-
516 dependent LTD is significantly decreased in CA3-CA1 components of the hippocampus of

517 *Fmr1*^{CRE} mutant mice as compare to wild type litter mate **(g-h) Olfactory function.** The mice
518 hemizygous for the variant in *Fmr1*^{CRE} showed a significant increase in time to discovery
519 compared to wildtype male controls in a buried food test. No significant difference in the
520 levels of latency to find food was observed in mice hemizygous for the variant in *Tenm1*^{CRE}
521 compared to wild type litter mates. i) **Audiogenic seizures.** No significant difference was
522 observed in audiogenic seizure incidence in the hemizygous mice with the variant *Fmr1*^{CRE}
523 compared to wild-type littermates. j) Pedigree of Family 347 of which individual S3 is a
524 member showing segregation of the mutation affecting *FMR1* expression.
525
526

References

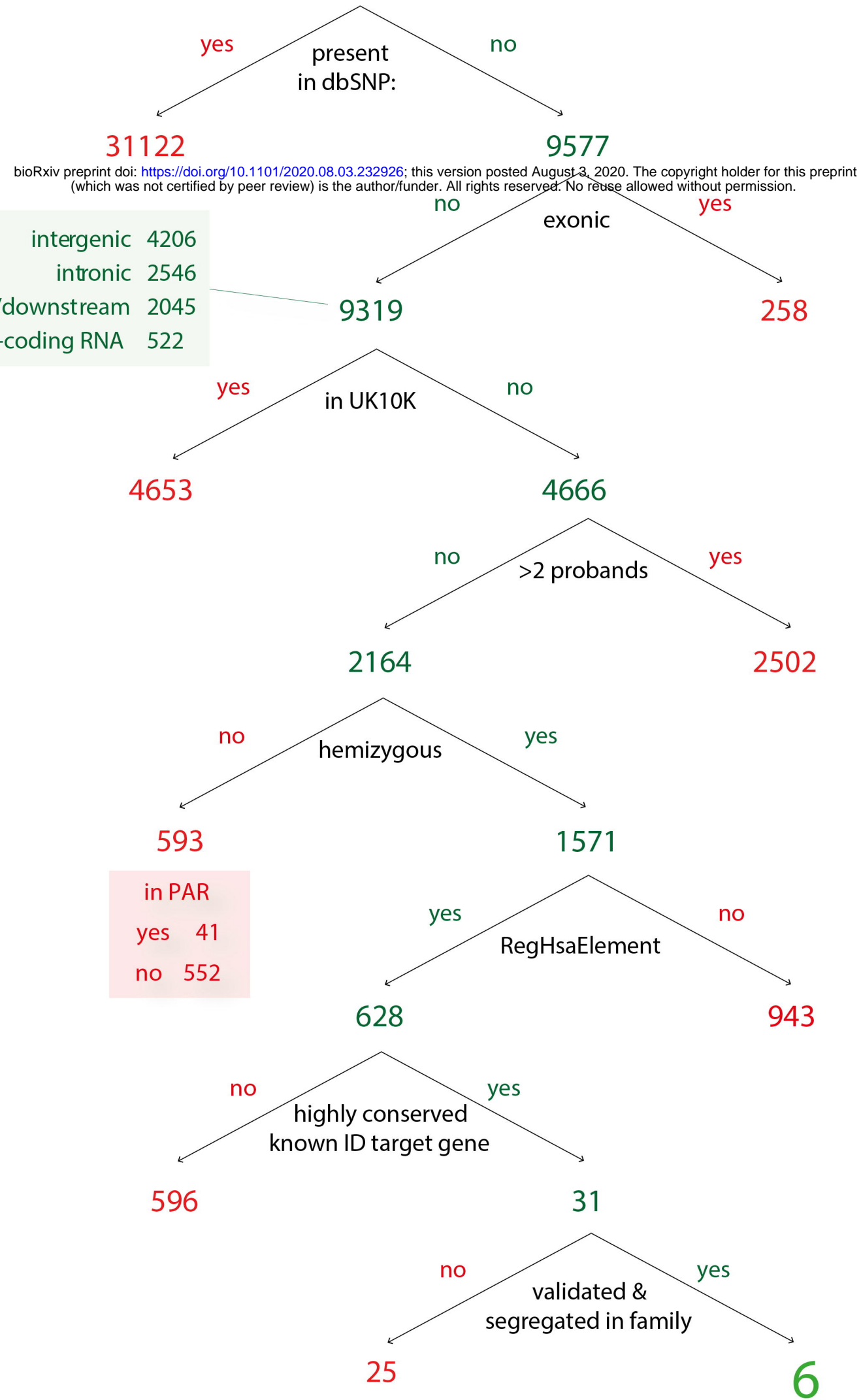
1. Thomas JW, *et al.* Comparative analyses of multi-species sequences from targeted genomic regions. *Nature* **424**, 788-793 (2003).
2. Kim TK, *et al.* Widespread transcription at neuronal activity-regulated enhancers. *Nature* **465**, 182-187 (2010).
3. Pradeepa MM, *et al.* Histone H3 globular domain acetylation identifies a new class of enhancers. *Nat Genet* **48**, 681-686 (2016).
4. Boyle AP, *et al.* High-resolution mapping and characterization of open chromatin across the genome. *Cell* **132**, 311-322 (2008).
5. Mifsud B, *et al.* Mapping long-range promoter contacts in human cells with high-resolution capture Hi-C. *Nat Genet* **47**, 598-606 (2015).
6. Calo E, Wysocka J. Modification of enhancer chromatin: what, how, and why? *Mol Cell* **49**, 825-837 (2013).
7. Kleinjan DA, van Heyningen V. Long-range control of gene expression: emerging mechanisms and disruption in disease. *Am J Hum Genet* **76**, 8-32 (2005).
8. Lettice LA, *et al.* Enhancer-adoption as a mechanism of human developmental disease. *Hum Mutat* **32**, 1492-1499 (2011).
9. Spielmann M, Lupianez DG, Mundlos S. Structural variation in the 3D genome. *Nat Rev Genet* **19**, 453-467 (2018).
10. Melo US, *et al.* Hi-C Identifies Complex Genomic Rearrangements and TAD-Shuffling in Developmental Diseases. *Am J Hum Genet*, (2020).
11. Hong JW, Hendrix DA, Levine MS. Shadow enhancers as a source of evolutionary novelty. *Science* **321**, 1314 (2008).
12. Deciphering Developmental Disorders S. Prevalence and architecture of de novo mutations in developmental disorders. *Nature* **542**, 433-438 (2017).
13. McEwen GK, Goode DK, Parker HJ, Woolfe A, Callaway H, Elgar G. Early evolution of conserved regulatory sequences associated with development in vertebrates. *PLoS Genet* **5**, e1000762 (2009).
14. Short PJ, *et al.* De novo mutations in regulatory elements in neurodevelopmental disorders. *Nature* **555**, 611-616 (2018).
15. MacArthur DG, *et al.* Guidelines for investigating causality of sequence variants in human disease. *Nature* **508**, 469-476 (2014).
16. Tarpey PS, *et al.* A systematic, large-scale resequencing screen of X-chromosome coding exons in mental retardation. *Nat Genet* **41**, 535-543 (2009).
17. Naville M, *et al.* Long-range evolutionary constraints reveal cis-regulatory interactions on the human X chromosome. *Nat Commun* **6**, 6904 (2015).
18. Whiffin N, *et al.* Using high-resolution variant frequencies to empower clinical genome interpretation. *Genet Med* **19**, 1151-1158 (2017).

19. Bhatia S, *et al.* Functional assessment of disease-associated regulatory variants in vivo using a versatile dual colour transgenesis strategy in zebrafish. *PLoS Genet* **11**, e1005193 (2015).
20. Inbal A, Kim SH, Shin J, Solnica-Krezel L. Six3 represses nodal activity to establish early brain asymmetry in zebrafish. *Neuron* **55**, 407-415 (2007).
21. Alkelai A, *et al.* A role for TENM1 mutations in congenital general anosmia. *Clin Genet* **90**, 211-219 (2016).
22. Osterweil EK, Krueger DD, Reinhold K, Bear MF. Hypersensitivity to mGluR5 and ERK1/2 leads to excessive protein synthesis in the hippocampus of a mouse model of fragile X syndrome. *J Neurosci* **30**, 15616-15627 (2010).
23. Hou L, Antion MD, Hu D, Spencer CM, Paylor R, Klann E. Dynamic translational and proteasomal regulation of fragile X mental retardation protein controls mGluR-dependent long-term depression. *Neuron* **51**, 441-454 (2006).
24. Amiri K, Hagerman RJ, Hagerman PJ. Fragile X-associated tremor/ataxia syndrome: an aging face of the fragile X gene. *Arch Neurol* **65**, 19-25 (2008).
25. Richards S, *et al.* Standards and guidelines for the interpretation of sequence variants: a joint consensus recommendation of the American College of Medical Genetics and Genomics and the Association for Molecular Pathology. *Genet Med* **17**, 405-424 (2015).
26. Tavtigian SV, *et al.* Modeling the ACMG/AMP variant classification guidelines as a Bayesian classification framework. *Genet Med* **20**, 1054-1060 (2018).
27. Brnich SE, *et al.* Recommendations for application of the functional evidence PS3/BS3 criterion using the ACMG/AMP sequence variant interpretation framework. *Genome Med* **12**, 3 (2019).
28. Stevenson RE, Schwartz CE. X-linked intellectual disability: unique vulnerability of the male genome. *Dev Disabil Res Rev* **15**, 361-368 (2009).
29. Piton A, Redin C, Mandel JL. XLID-causing mutations and associated genes challenged in light of data from large-scale human exome sequencing. *Am J Hum Genet* **93**, 368-383 (2013).
30. Benko S, *et al.* Highly conserved non-coding elements on either side of SOX9 associated with Pierre Robin sequence. *Nat Genet* **41**, 359-364 (2009).
31. Bhatia S, *et al.* Disruption of autoregulatory feedback by a mutation in a remote, ultraconserved PAX6 enhancer causes aniridia. *Am J Hum Genet* **93**, 1126-1134 (2013).
32. Nordeen SK. Luciferase reporter gene vectors for analysis of promoters and enhancers. *Biotechniques* **6**, 454-458 (1988).
33. Bodaleo F, Tapia-Monsalves C, Cea-Del Rio C, Gonzalez-Billault C, Nunez-Parra A. Structural and Functional Abnormalities in the Olfactory System of Fragile X Syndrome Models. *Front Mol Neurosci* **12**, 135 (2019).
34. Juncos JL, *et al.* Olfactory dysfunction in fragile X tremor ataxia syndrome. *Mov Disord* **27**, 1556-1559 (2012).
35. Dahlhaus R. Of Men and Mice: Modeling the Fragile X Syndrome. *Front Mol Neurosci* **11**, 41 (2018).

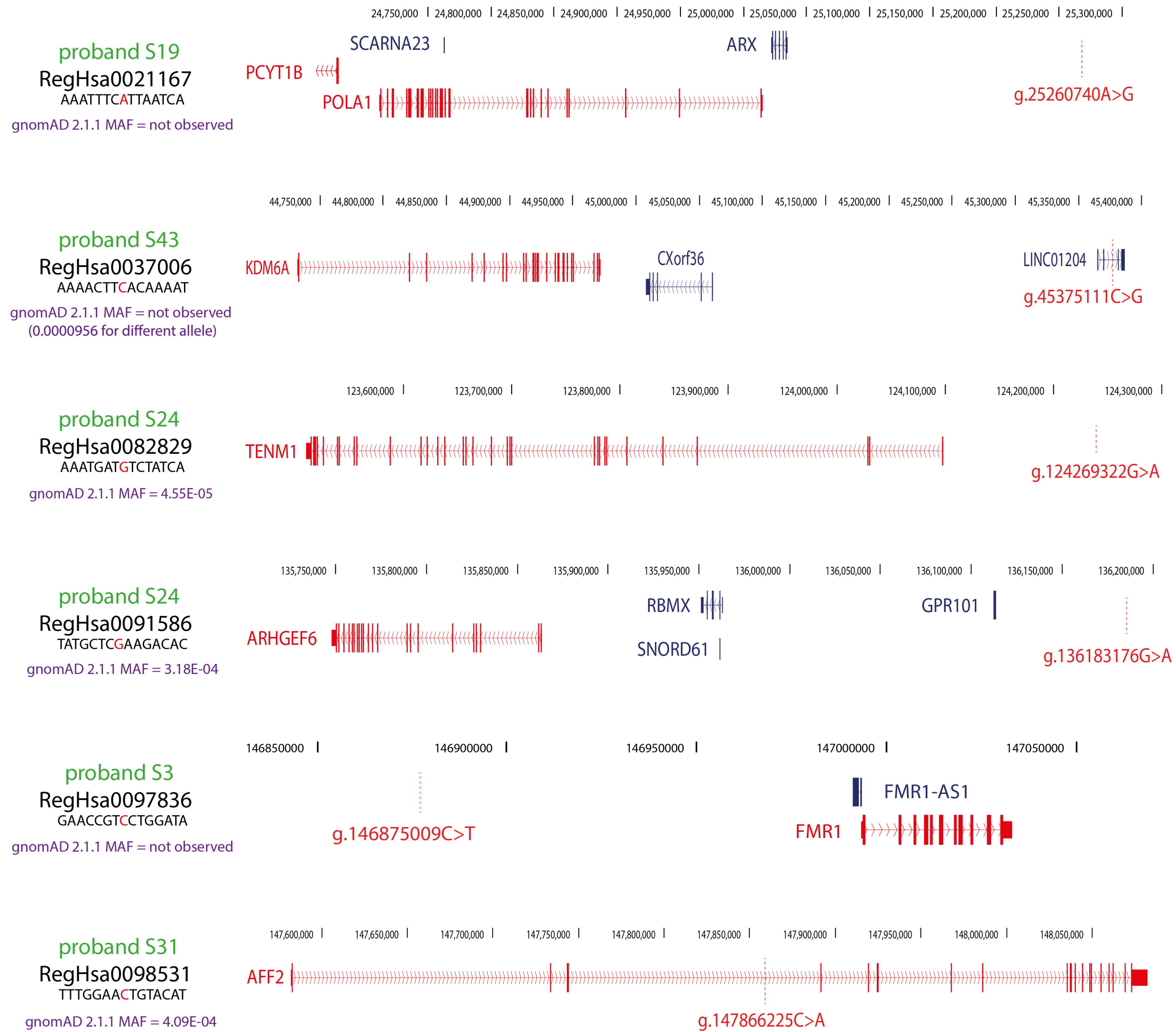
36. Prabhakar S, *et al.* Human-specific gain of function in a developmental enhancer. *Science* **321**, 1346-1350 (2008).
37. Li H, Durbin R. Fast and accurate long-read alignment with Burrows-Wheeler transform. *Bioinformatics* **26**, 589-595 (2010).
38. DePristo MA, *et al.* A framework for variation discovery and genotyping using next-generation DNA sequencing data. *Nat Genet* **43**, 491-498 (2011).
39. Cingolani P, *et al.* A program for annotating and predicting the effects of single nucleotide polymorphisms, SnpEff: SNPs in the genome of *Drosophila melanogaster* strain w1118; iso-2; iso-3. *Fly (Austin)* **6**, 80-92 (2012).
40. Grant CE, Bailey TL, Noble WS. FIMO: scanning for occurrences of a given motif. *Bioinformatics* **27**, 1017-1018 (2011).
41. Carlin D, Sepich D, Grover VK, Cooper MK, Solnica-Krezel L, Inbal A. Six3 cooperates with Hedgehog signaling to specify ventral telencephalon by promoting early expression of *Foxg1a* and repressing *Wnt* signaling. *Development* **139**, 2614-2624 (2012).
42. Thisse C, Thisse B. High-resolution in situ hybridization to whole-mount zebrafish embryos. *Nat Protoc* **3**, 59-69 (2008).
43. Hecksher-Sorensen J, Hill RE, Lettice L. Double labeling for whole-mount in situ hybridization in mouse. *Biotechniques* **24**, 914-916, 918 (1998).
44. Thomson SR, *et al.* Cell-Type-Specific Translation Profiling Reveals a Novel Strategy for Treating Fragile X Syndrome. *Neuron* **95**, 550-563 e555 (2017).
45. Barnes SA, *et al.* Convergence of Hippocampal Pathophysiology in *Syngap*^{+/-} and *Fmr1*^{-/y} Mice. *J Neurosci* **35**, 15073-15081 (2015).

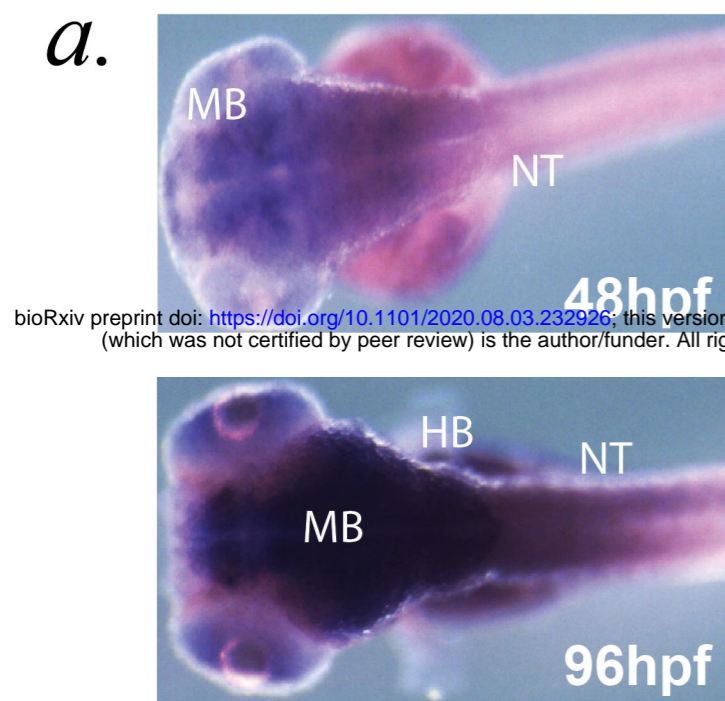
a.

40699 total variants

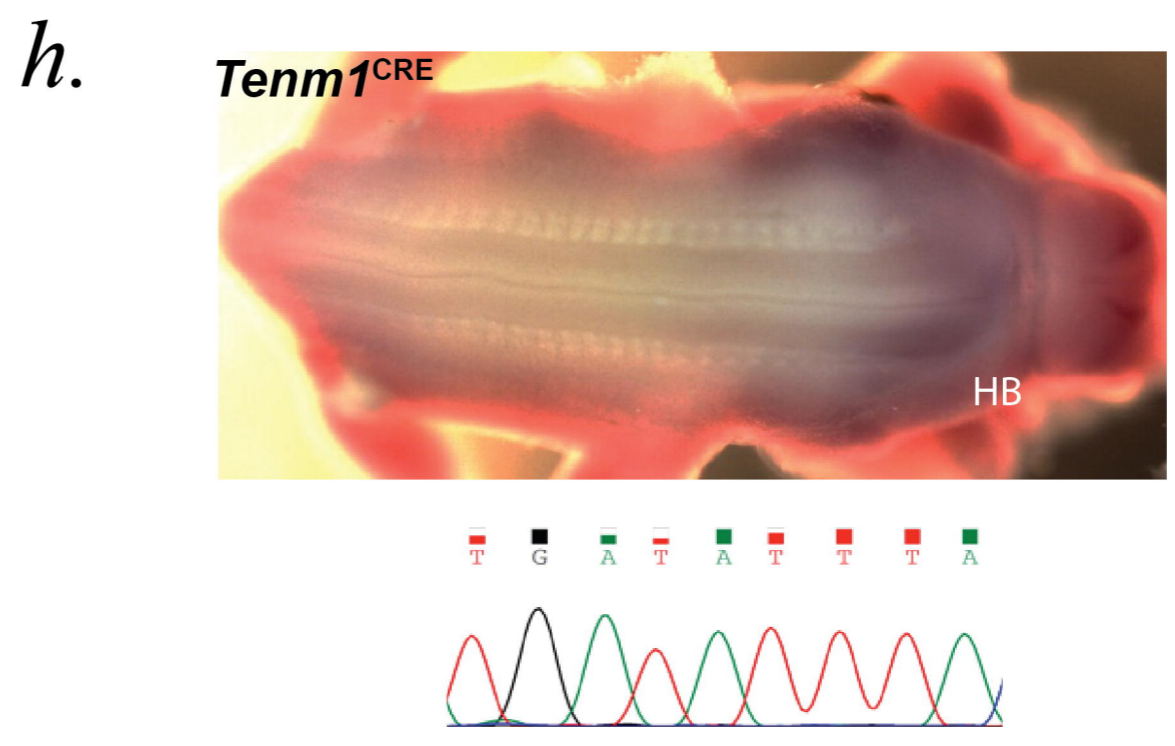
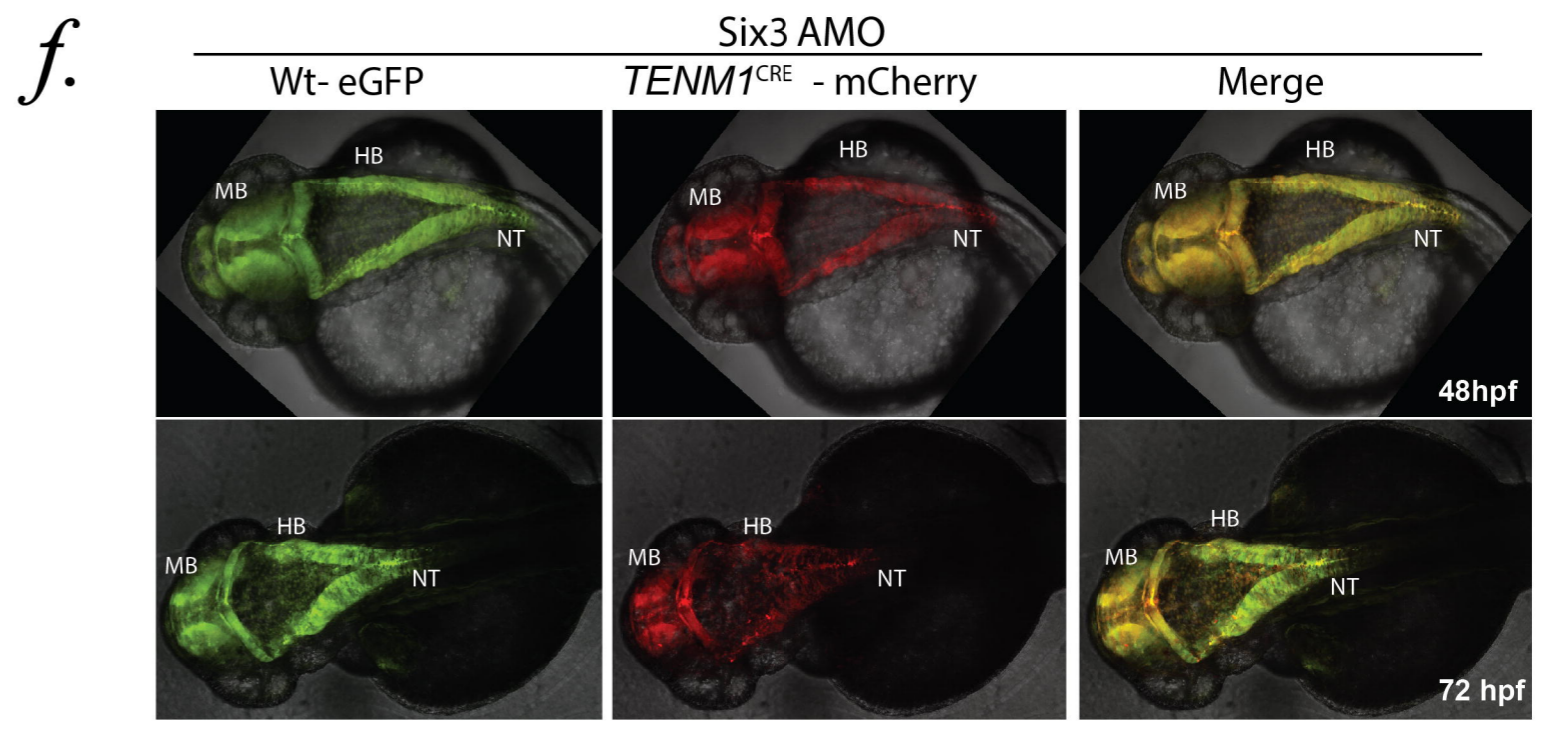
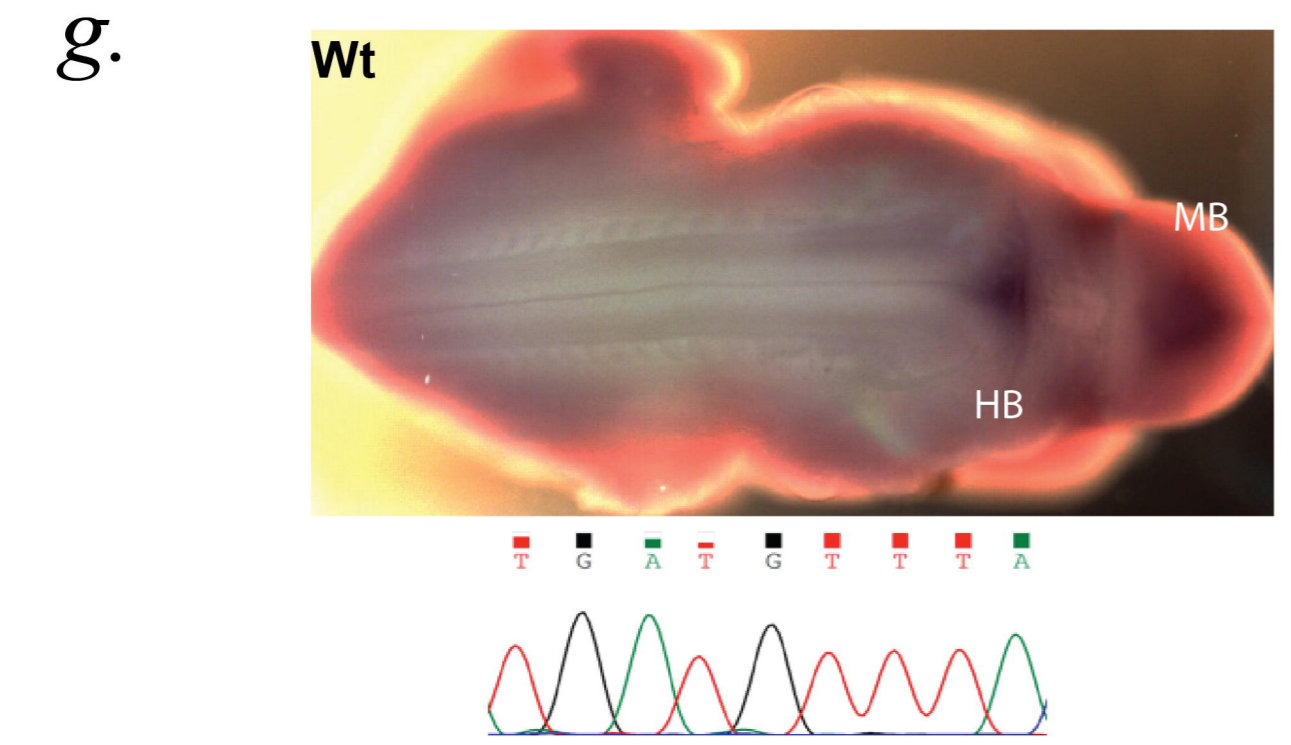
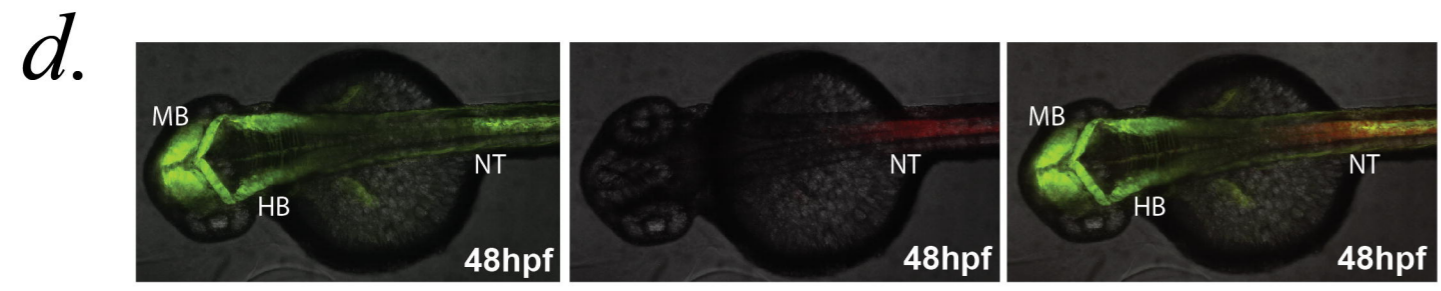
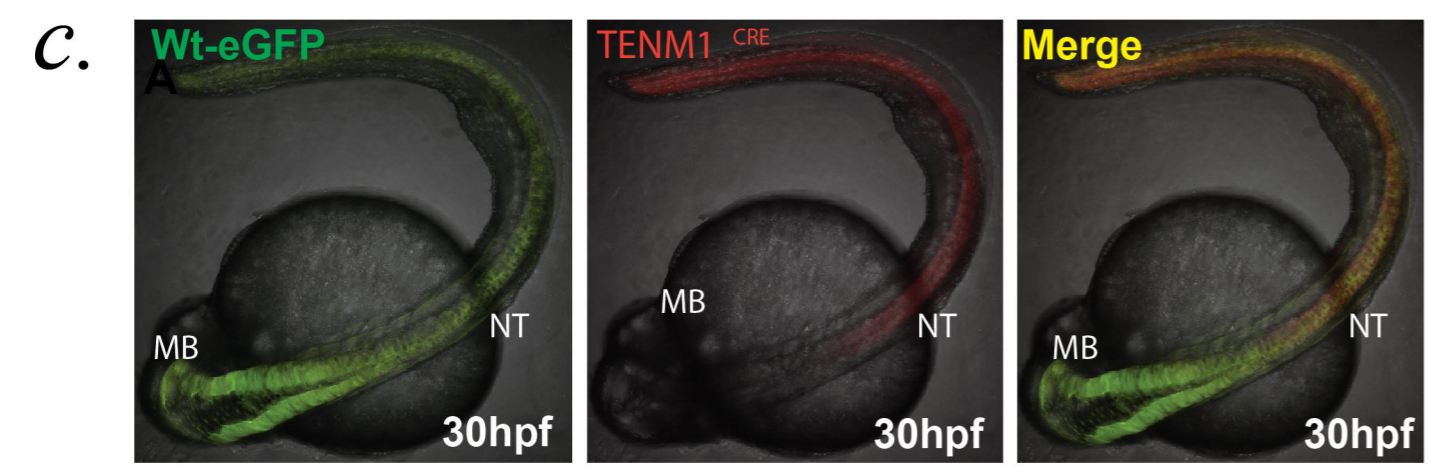
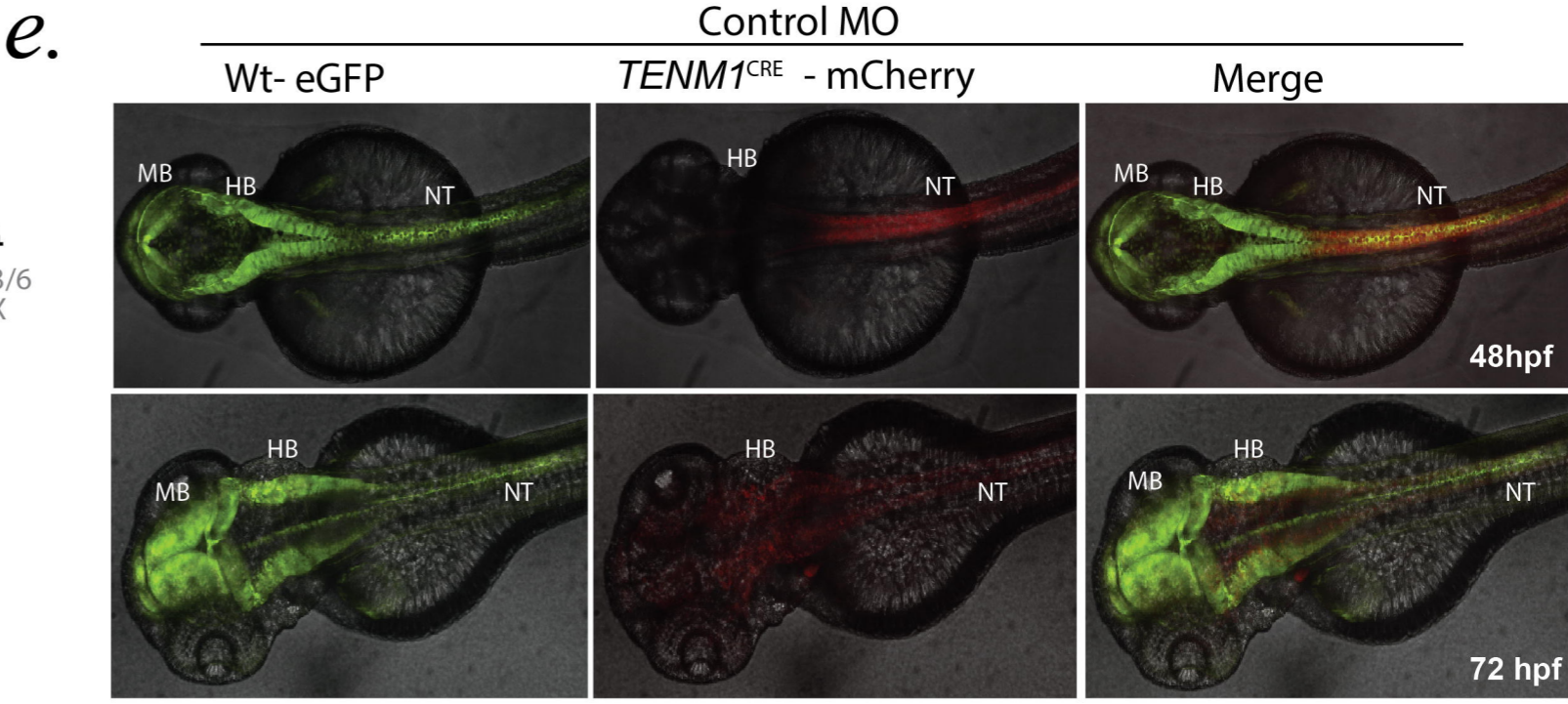
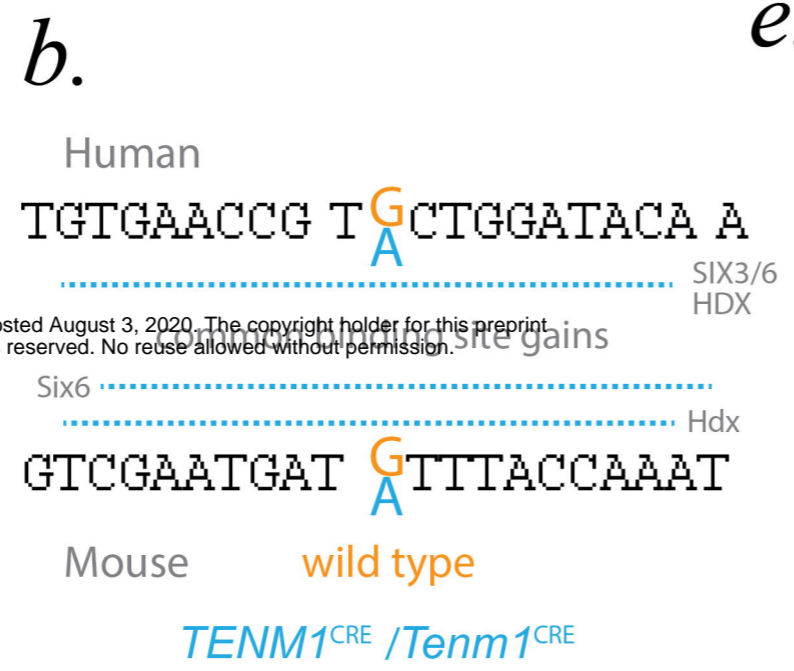


b.

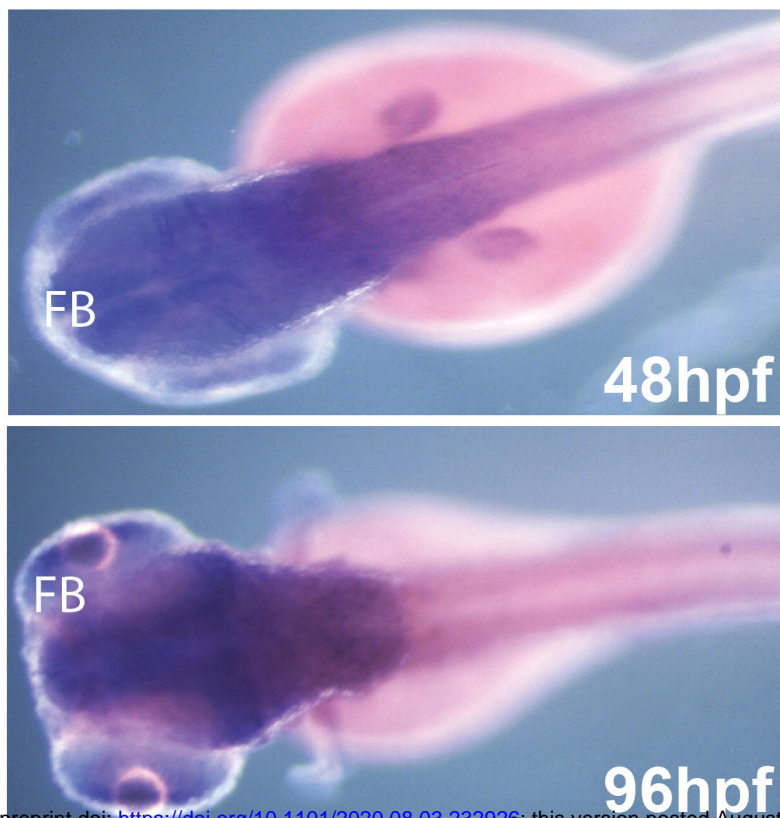




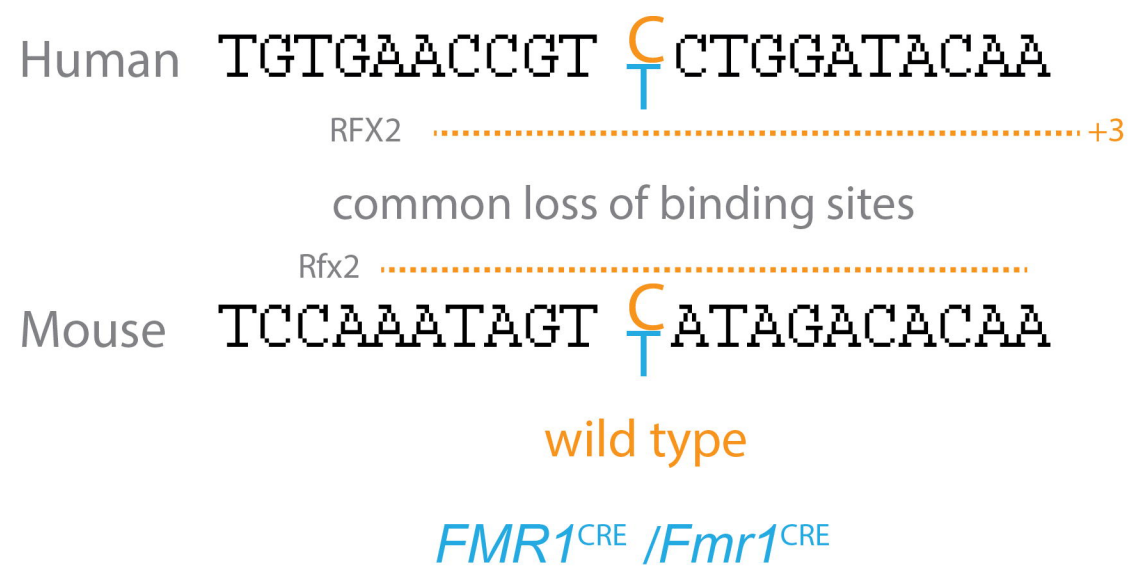
bioRxiv preprint doi: <https://doi.org/10.1101/2020.08.03.232926>; this version posted August 3, 2020. The copyright holder for this preprint (which was not certified by peer review) is the author/funder. All rights reserved. No reuse allowed without permission.



a.

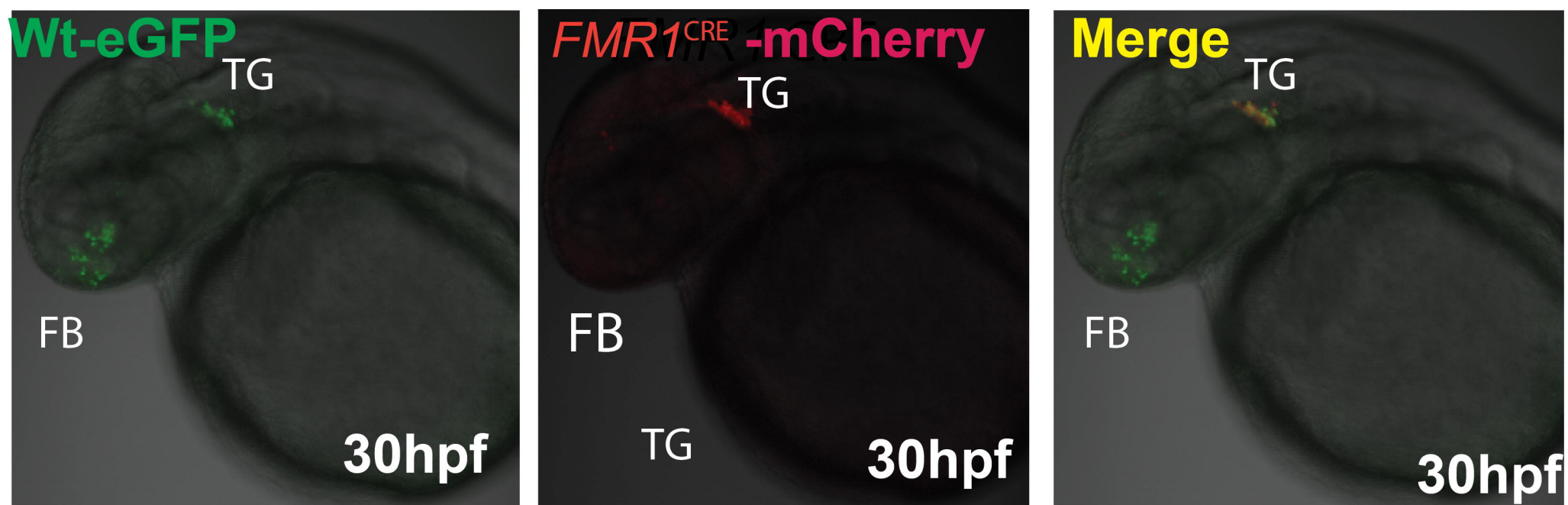


b.

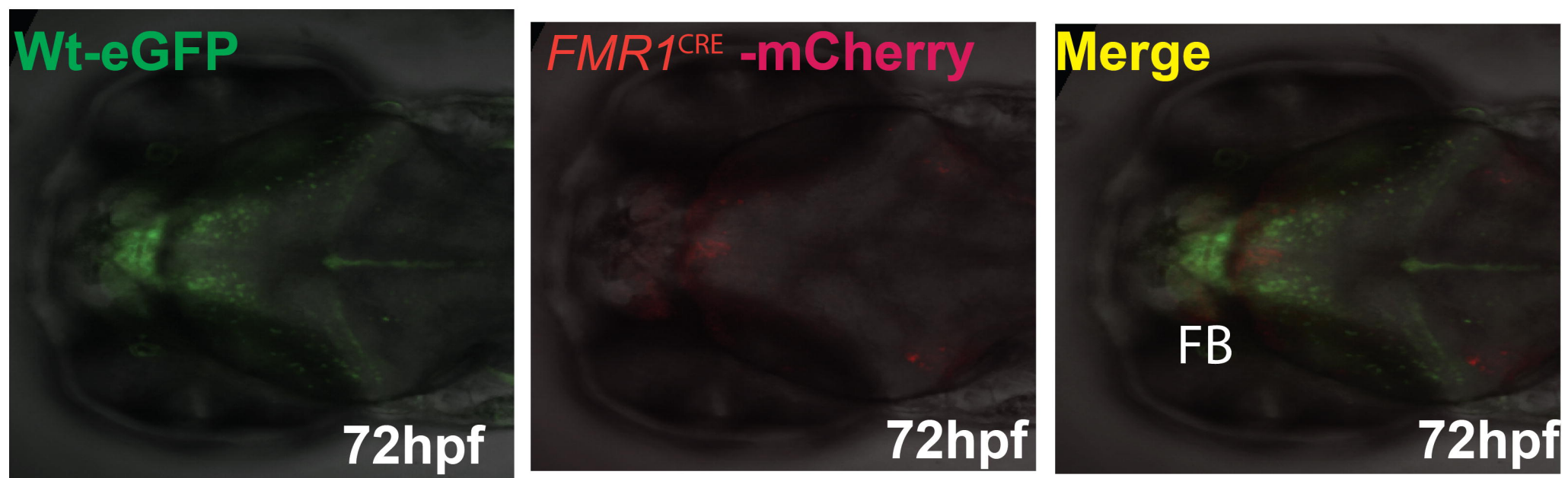


bioRxiv preprint doi: <https://doi.org/10.1101/2020.08.03.232926>; this version posted August 3, 2020. The copyright holder for this preprint (which was not certified by peer review) is the author/funder. All rights reserved. No reuse allowed without permission.

c.



d.



e.

